Design Proposal Report: Analysis of Mach-Zehnder Interferometer

KOMAL GUPTA[1,*]

[1]*Institute of Photonics Technologies, National Tsing Hua University, Hsinchu, Taiwan 300*
**komalgupta@gapp.nthu.edu.tw*

Abstract: This report presents a study of a Mach-Zehnder Interferometer (MZI) on a silicon-on-insulator (SOI) platform. The investigation includes an analysis of waveguide propagation modes, variations in effective index, and group index. Additionally, the simulated transfer function, transmission characteristics, and free spectral range (FSR) calculations are examined for an imbalanced MZI. A preliminary layout mask is also introduced for potential fabrication and further analysis.

1. Introduction

Integrated photonic devices based on silicon-on-insulator (SOI) platforms have gained significant attention due to their compact footprint, CMOS compatibility, and high-performance optical characteristics [1-3]. Among these devices, Mach-Zehnder interferometers (MZIs) are widely used for sensing, modulation, and filtering applications due to their precise phase-dependent interference. However, optimizing MZI performance requires careful analysis of waveguide properties, including propagation modes, effective index, and group index, as well as the spectral response under imbalanced path conditions.

This work investigates an SOI-based MZI, examining its modal behavior and refractive index variations to understand their influence on device functionality. Through simulations, the transfer function, transmission spectrum, and free spectral range (FSR) for different path length imbalances was evaluated, providing insights into design trade-offs for targeted applications. Additionally, a preliminary mask layout to facilitate future fabrication and experimental validation is presented.

2. Theory

The operation of a Mach-Zehnder interferometer (MZI) on a silicon-on-insulator (SOI) platform can be comprehensively described through electromagnetic wave propagation theory [4]. Figure. 1 shows a schematic of a simple MZI. When light enters the input Y-junction, the electric field E_{in} is equally divided into two arms, expressed as $E_1 = E_{in}e^{(i\beta_1 L_1)}/\sqrt{2}$ and $E_2 = E_{in}e^{(i\beta_2 L_2)}/\sqrt{2}$, where $\beta = 2\pi n_{eff}/\lambda$ represents the propagation constant, n_{eff} is the waveguide's effective refractive index, and L_1 and L_2 denote the lengths of the two interferometer arms. The path length difference is equally divided into two arms, expressed as $\Delta L = L_2 - L_1$ introduces a critical phase shift $\Delta\phi = \beta\Delta L$ between the two arms, which fundamentally determines the interferometer's behavior. For a Y-branch splitter, $E_1 = E_2 = E_{in}/\sqrt{2}$.

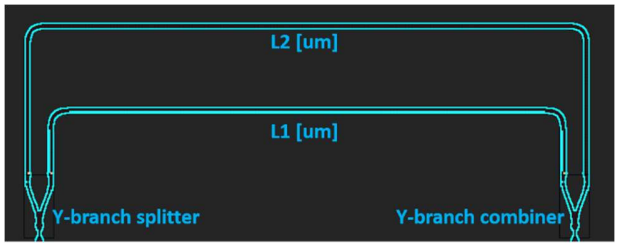

Figure 1. Schematic of a simple MZI.

The output of the Y- branch combiner for a lossless imbalanced MZI with $\beta_1 = \beta_2 = \beta$ is given by E_o (equation 1) and the corresponding transfer function is given by I_o (equation 2).

$$E_o = \frac{E_{in}}{2}\left(e^{(-i\beta_1 L_1)} + e^{(-i\beta_2 L_2)}\right) \quad (1)$$

$$I_o = \frac{I_{in}}{2}\left[1 + \cos(\beta \Delta L)\right] \quad (2)$$

The above relationship reveals the periodic nature of the MZI's transmission function, where constructive and destructive interference occur at specific phase differences. The periodicity of this interference pattern is characterized by the free spectral range (FSR), given by

$$FSR = \frac{\lambda^2}{n_g(\lambda)\,\Delta L} \quad (3)$$

where n_g is the group index defined by

$$n_g(\lambda) = n_{eff}(\lambda) - \lambda \frac{dn_{eff}(\lambda)}{d\lambda} \quad (4)$$

which accounts for waveguide dispersion effects. The group index plays a crucial role in determining the wavelength-dependent performance of the device, particularly in broadband applications. Practical implementations consider propagation losses, which modify the ideal transfer function. When accounting for attenuation coefficient α, the transmission becomes

$$I_o = \frac{I_{in}}{4}\left[e^{(-i\alpha_1 L_1)} + e^{(-i\alpha_2 L_2)} + 2e^{-\frac{\alpha_1 L_1 + \alpha_2 L_2}{2}}\cos(\beta \Delta L)\right] \quad (5)$$

This more complete expression demonstrates how fabrication imperfections and material losses influence the device's performance. The effective index $n_{eff}(\lambda)$, which depends on the waveguide geometry and material properties, can be determined through numerical mode-solving techniques, while the group index n_g provides insight into the device's dispersion characteristics. Together, these parameters enable precise engineering of the MZI's spectral response for applications in optical filtering, modulation, and sensing. The theoretical framework presented here forms the basic foundation for designing imbalanced MZI devices in SOI platforms.

3. Modeling and Simulations

3.1 Waveguide Modeling

The strip waveguide structure was simulated using Lumerical MODE Solver, with cross-sectional dimensions of 220 nm (height) × 550 nm (width) which is a standard specification adopted by major silicon photonics foundries. Modal analysis was conducted at the wavelength of 1550 nm to characterize the guided modes. Figure 2(a) shows the simulated transverse electric (TE) mode profile, while Figure 2(b) shows the corresponding transverse magnetic (TM) mode distribution, clearly illustrating the distinct field confinement characteristics for each polarization state.

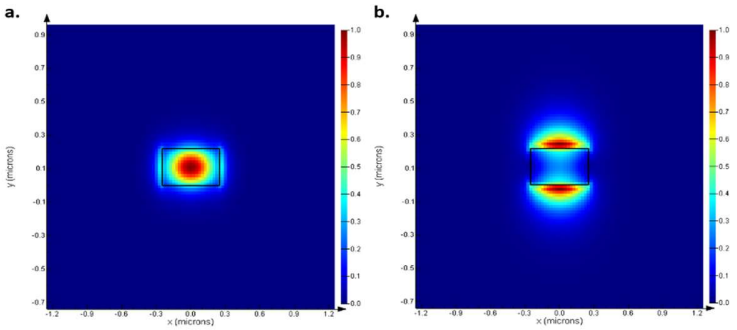

Figure 2. Simulated mode profiles (a) TE and (b) TM.

The wavelength-dependent characteristics of the fundamental TE mode were investigated through systematic parameter sweeps. Figure 3 presents the spectral analysis results, where (a) shows the wavelength dependence of both real and imaginary components of the effective refractive index, while (b) displays the corresponding group index variations across the 1500-1600 nm wavelength range. The real part of the effective index exhibits characteristic normal dispersion behavior, decreasing monotonically with increasing wavelength, while the imaginary component reveals wavelength-dependent propagation losses. The group index demonstrates a gradual reduction across the spectrum, consistent with the known dispersion properties of silicon waveguides in this spectral region.

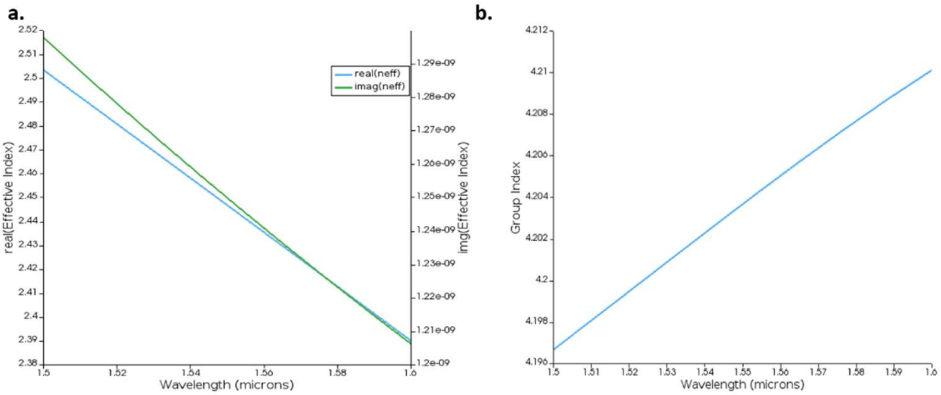

Figure 3. Wavelength dependence of (a) effective index and (b) group index for TE mode.

For designing the compact waveguide model supporting the TE mode, the wavelength dependence of the effective index was analytically represented through Taylor series expansion (equation 6), with the corresponding coefficients systematically determined. The fitted equation takes the form

$$n_{eff}(\lambda) = n_0 + n_1(\lambda - \lambda_0) + n_3(\lambda - \lambda_0)^2 \quad (6)$$

$$\Rightarrow n_{eff}(\lambda) = 2.44682 - 1.13339(\lambda - \lambda_0) - 0.0439(\lambda - \lambda_0)^2 \quad (7)$$

where n_0 represents the effective index at the central wavelength λ_0 = 1550 nm, and the higher-order terms capture the dispersion characteristics. Figure 4 demonstrates excellent agreement between the numerically calculated effective indices (discrete points) and the Taylor series approximation (solid curve), validating the accuracy of this compact model.

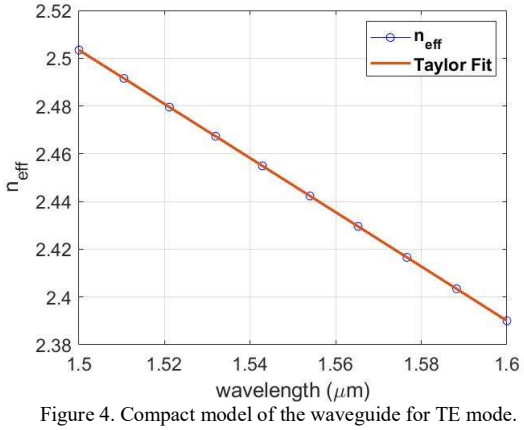

Figure 4. Compact model of the waveguide for TE mode.

The compact waveguide model was employed to numerically simulate the transfer function of an imbalanced MZI through MATLAB. Figure 5 presents the comprehensive simulation results. Figure 5 (a) and (b) depict the spectral transmission characteristics in linear scale and logarithmic (dB) scale respectively, revealing the periodic wavelength-dependent interference pattern. The complementary analysis in (c) and (d) demonstrates the MZI's transmission response as a function of path length difference (ΔL) at the design wavelength of 1550 nm, showing the expected sinusoidal dependence of the interferometric output on the optical phase difference.

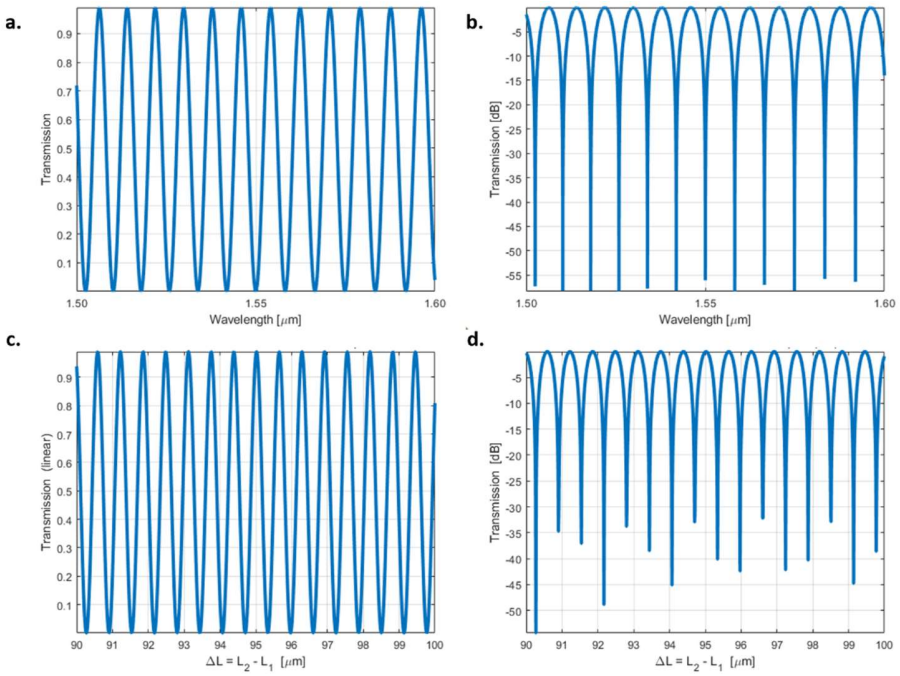

Figure 5. MZI transmission characteristics: Wavelength dependence (a) linear and (b) dB scale. ΔL dependence at 1550 nm (c) linear scale and (d) dB scale.

3.2 MZI Modeling and Simulations

The MZI structure incorporating Y-branches (as splitter and combiner) with varying path length differences (ΔL) was simulated using Lumerical INTERCONNECT to systematically investigate its spectral characteristics. Figure 6 presents the simulation results, where (a)-(c) display the TE mode gain in dB scale for three distinct ΔL values, while panels (d)-(f) show the corresponding transmission spectra. This parametric study was specifically designed to achieve targeted FSR within 1-20 nm by controlling the optical path difference, while maintaining optimal power splitting efficiency through the Y-junctions. The consistent waveguide geometry (220 nm × 550 nm) and single-mode operation at 1550 nm ensures comparable modal properties across all designs, enabling clear observation of how ΔL modification affects both the spectral periodicity (FSR) and insertion loss characteristics of the MZI devices.

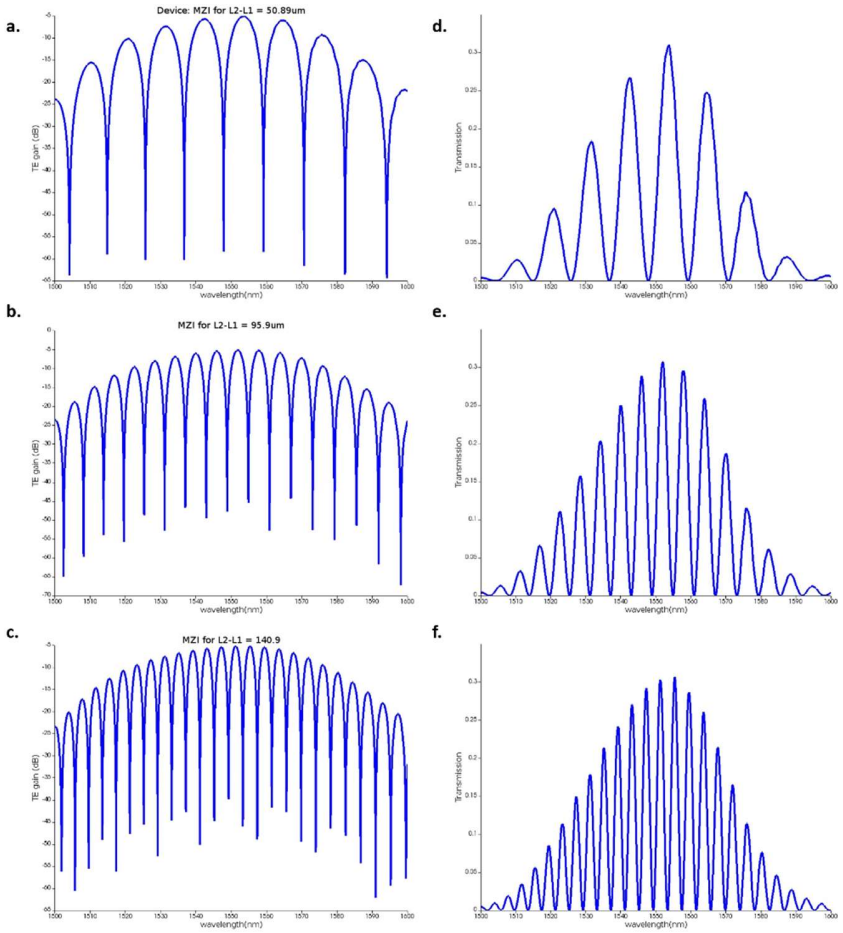

Figure 6. Numerical simulation of MZI performance with varied path length differences (ΔL): (a-c) TE mode gain (dB scale) and (d-f) corresponding transmission spectra.

The theoretically calculated FSR values from equation (3) were systematically compared with the simulated MZI responses to validate the analytical model. Table 1 presents this comparative study, demonstrating excellent agreement between the predicted and simulated FSR values across different path length differences (ΔL). The verification process confirms the accuracy of both the waveguide dispersion model and the MZI transfer function implementation.

Table 1. FSR for different ΔL

ΔL (μm)	FSR Theoretical	FSR Simulated
50.89	11 nm	11.082 nm
95.9	5.94 nm	6.09 nm
140.9	4.04 nm	4.12 nm

Following successful simulation results, the proposed MZI designs were translated into fabrication-ready layouts using KLayout. Figure 7 presents the complete schematic of the three MZI implementations, incorporating specific design features to facilitate automated optical

testing. The layout incorporated two critical constraints to ensure compatibility with the measurement setup: (1) all TE grating couplers were oriented toward the right side of the chip to eliminate the need for rotational alignment during testing, and (2) a fixed 127 μm pitch was maintained for both input and output grating couplers to precisely match the fiber array configuration of the automated probe station.

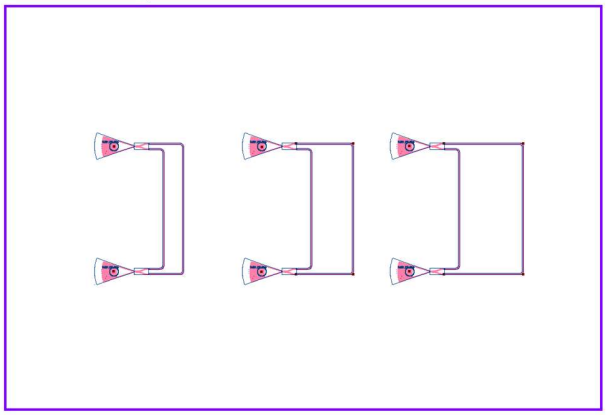

Figure 7. Proposed layout of the three different MZI(s).

4. Conclusions

This report presents the design and analysis of three Mach-Zehnder interferometers (MZIs) implemented using silicon strip waveguides with varying path lengths. The study systematically investigates the waveguide modal characteristics, effective index dispersion, and spectral performance of imbalanced MZI configurations. Through numerical simulations and theoretical modeling, the designs were optimized to achieve target free spectral ranges (FSR) while maintaining compatibility with standard silicon photonics fabrication processes. The proposed layouts incorporate test-optimized features including right-oriented grating couplers and 127 μm pitch for automated characterization.

References

1. H. Subbaraman, X. C. Xu, A. Hosseini et al., "Recent advances in silicon-based passive and active optical interconnects," Opt Express **23**, 2487-2510 (2015).
2. Michal Lipson, "Guiding, Modulating, and Emitting Light on Silicon-Challenges and Opportunities," J. Lightwave Technol. 23, 4222- (2005)
3. Bogaerts, W., De Heyn, P., Van Vaerenbergh, T., De Vos, K., Kumar Selvaraja, S., Claes, T., Dumon, P., Bienstman, P., Van Thourhout, D. and Baets, R. (2012), Silicon microring resonators. Laser & Photon. Rev., 6: 47-73.
4. Chrostowski L, Hochberg M. Silicon Photonics Design: From Devices to Systems. Cambridge University Press; 2015.